ACS APPLIED MATERIALS & INTERFACES

Research Article

www.acsami.org

Coordination-Enabled One-Step Assembly of Ultrathin, Hybrid Microcapsules with Weak pH-Response

Chen Yang,[†,§] Hong Wu,[†,§] Xiao Yang,[†,§] Jiafu Shi,[*,‡,§] Xiaoli Wang,[†,§] Shaohua Zhang,[†,§] and Zhongyi Jiang[*,†,§]

[†]Key Laboratory for Green Chemical Technology of Ministry of Education, School of Chemical Engineering and Technology and [‡]School of Environmental Science and Engineering, Tianjin University, Tianjin 300072, China

[§]Collaborative Innovation Center of Chemical Science and Engineering (Tianjin), Tianjin 300072, China

Supporting Information

ABSTRACT: In this study, an ultrathin, hybrid microcapsule is prepared though coordination-enabled one-step assembly of tannic acid (TA) and titanium(IV) bis(ammonium lactate) dihydroxide (Ti-BALDH) upon a hard-templating method. Briefly, the PSS-doped $CaCO_3$ microspheres with a diameter of 5−8 μm were synthesized and utilized as the sacrificial templates. Then, TA-Ti^{IV} coatings were formed on the surface of the PSS-doped $CaCO_3$ templates through soaking in TA and Ti-BALDH aqueous solutions under mild conditions. After removing the template by EDTA treatment, the TA-Ti^{IV} microcapsules with a capsule wall thickness of 15 ± 3 nm were obtained. The strong coordination bond between polyphenol and Ti^{IV} conferred the TA-Ti^{IV} microcapsules high structural stability in the range of pH values 3.0−11.0. Accordingly, the enzyme-immobilized TA-Ti^{IV} microcapsules exhibited superior pH and thermal stabilities. This study discloses the formation of TA-Ti^{IV} microcapsules that are suitable for use as supports in catalysis due to their extensive pH and thermal stabilities.

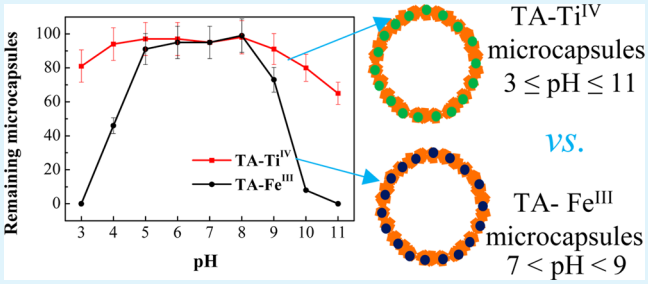

KEYWORDS: *metal−organic coordination, hybrid materials, microcapsules, weak pH-response, enzyme catalysis*

1. INTRODUCTION

Microcapsules, attributed to the hollow structure and tunable wall structures, have attracted great attentions from diverse applications such as drug/gene delivery, catalysis, sensors, etc.[1−4] Till now, several methods have been exploited to prepare microcapsules, including layer-by-layer (LbL) self-assembly, the sol−gel method, interfacial polymerization/reaction, etc.[5] Among these, LbL self-assembly is regarded as one of the most commonly used method.[6] In earlier research, the LbL self-assembly process for preparing microcapsules is primarily performed through the alternative deposition of different materials (building blocks) on sacrificial templates upon electrostatic attraction or hydrogen bonding.[7] Multiple adsorption/washing cycles are often required to obtain desirable capsule structures with sufficient mechanical stability. To enhance the structural stability, some post-treatment approaches such as chemical cross-linking, nanohybridization, etc., are often needed.[8,9] According to the stimuli-responsive behavior, LbL microcapsules can be classified into pH-responsive and weak pH-responsive microcapsules. For pH-responsive microcapsules, Caruso and co-workers reported the preparation of poly(L-glutamic acid) and poly(L-lysine) PGA/PLL films on mesoporous silica templates through electrostatic force, which were sensitive to pH.[10] These pH-responsive microcapsules may not be very suitable in some specific applications, such as catalysis. Weak pH-responsive microcapsules that could keep their wall structure unchanged or only slightly changed over a wide pH range are highly anticipated since they could well isolate the encapsulated cargoes from bulk solution without leaching. So far, there are two major strategies have been explored to prepare weak pH-responsive microcapsules (i) shielding the outermost polyelectrolyte layer of the noncovalent multilayered hollow microspheres and (ii) linking the layers with the strong interactions to form the covalent multilayers.[11] Although tremendous efforts have been input, developing a facile and mild approach to preparing microcapsules with weak pH-response is still urgently required.

In general, coordination bonding energy (200−400 kJ/mol) is stronger than hydrogen bonding energy (5−30 kJ/mol) and electrostatic force (50−200 kJ/mol).[12] Thus, coordination-enabled assembly might render a simple and convenient approach for the fabrication of weak pH-responsive microcapsules. In these years, a number of researchers have also devoted great efforts to explore more facile and controllable approaches to the preparation of microcapsules. As one of most representative examples, Caruso and co-workers developed a

Received: February 13, 2015
Accepted: April 21, 2015
Published: April 21, 2015

DOI: 10.1021/acsami.5b01463
ACS Appl. Mater. Interfaces 2015, 7, 9178−9184

rapid, one-step assembly process based upon tannic acid-Fe ($TA\text{-}Fe^{III}$) coordination reaction to form hybrid microcapsules under mild conditions (aqueous solution, neutral pH, room temperature).[13] The resultant $TA\text{-}Fe^{III}$ microcapsules showed great potential in drug/gene delivery in vivo as a result of pH-sensitive disassembly behavior.[14] To acquire weak pH-responsive microcapsules, it is still crucial to screen out suitable pair of metal ion and organic ligand, which could form robust coordination bond. Organic ligands with catechol groups could establish stable coordination bond in aqueous solution because of the formation of five-membered chelate rings. On the other hand, the first-row transition metal ions could coordinate with catechol or its derivatives. Metal ions with stable high oxidation state (i.e., Ti^{IV}, Fe^{III}, Cr^{III}) could coordinate with catechol primarily through a tris-coordination state, possessing a larger equilibrium constant. The divalent metal ions (i.e., Cu^{II}, Ni^{II}, Cr^{II}) could coordinate with catechol only through mono- and bis-coordination states.[15,16] It is deductive that the higher the oxidation state of the metal ions, the more stable the coordination bond would be. (The formula ($Charge^2$/Radius) could be used to roughly assess the stability of coordination compounds, and corresponding information about the stability of some common metal ions was summarized and compared in Figure S1.) Ti is then considered as a preferential choice to fabricate weak pH-responsive metal−organic coordination compounds because of its higher valence state, low cost, low toxicity, and pH corrosion resistance.[17] Thus, it is conjectured that a weak pH-sensitive coordination bond can be formed between Ti and catechol-containing organic ligands, which will confer the resultant microcapsules with a weak pH-responsive property.

Herein, we presented the first example of coordination-enabled synthesis of $TA\text{-}Ti^{IV}$ ultrathin microcapsules with weak pH-response. Specifically, the PSS-doped $CaCO_3$ microspheres with a diameter of 5−8 μm were synthesized and utilized as the sacrificial templates.[18] Then, $TA\text{-}Ti^{IV}$ coatings were formed on the surface of the PSS-doped $CaCO_3$ templates through soaking in TA and titanium(IV) bis (ammonium lactate) dihydroxide (Ti-BALDH) aqueous solutions under mild conditions. Finally, the $TA\text{-}Ti^{IV}$ microcapsules were obtained after removing the templates through EDTA treatment. For comparison purposes, the $TA\text{-}Fe^{III}$ microcapsules were simultaneously investigated.

2. EXPERIMENTAL SECTION

2.1. Materials. Tannic acid (TA, ACS reagent), poly(sodium 4-styrenesulfonate) (PSS, $M_w \sim 70\,000$), fluorescein isothiocyanate (FITC), titanium(IV) bis (ammonium lactate) dihydroxide (Ti-BALDH, 50 wt. % aqueous solution), Na_2CO_3, $CaCl_2{\cdot}2H_2O$, $NaH_2PO_4{\cdot}2H_2O$, $Na_2HPO_4{\cdot}12H_2O$, and Catalase (CAT, 2000−5000 units mg^{-1} protein EC.1.11.1.6) were purchased from Sigma-Aldrich. Hydrogen peroxide (H_2O_2, 30 wt %) was obtained from Tianjin Guangfu Fine Chemical Research Institute (Tianjin, China). Fluorescent-labeled CAT was prepared by incubating the mixtures of FITC and CAT (50 mM phosphate buffer, pH 8.0, CAT concentration 2 mg mL^{-1}, [FITC]/[CAT] = 5) at room temperature for 24 h. Then, exhaustively dialyze through a dialysis bag (M_w cutoff 14 000) against phosphate buffer (50 mM, pH 7.0) for 72 h and deionized water for 24 h. High-purity water with a resistivity of 18.2 MΩ.cm was obtained from the Millipore Milli-Q purification system.

2.2. Preparation of PSS-Doped $CaCO_3$ Microspheres. All solutions were newly prepared for immediate use. The $CaCl_2$ solution was prepared by dissolving $CaCl_2{\cdot}2H_2O$ (0.33 mM, 970 mg) in 20 mL demineralized H_2O. Then, the Na_2CO_3 solution with the same concentration was prepared by dissolving Na_2CO_3 (0.33 mM, 700 mg) in 20 mL demineralized H_2O. After that, 40 mg PSS was added in Na_2CO_3 solution. Finally, $CaCl_2$ and PSS-Na_2CO_3 solution were mixed and stirred vigorously for 30 s. The newly synthesized white PSS-doped $CaCO_3$ microspheres were centrifuged with 724 g for 3 min and washed with water three times.

2.3. Preparation of the $TA\text{-}Ti^{IV}$ Microcapsules. The standard preparation process was described as follows: the as-prepared PSS-doped $CaCO_3$ microspheres were dispersed in 5 mL demineralized H_2O, 2/5 of which were added into 12 mL H_2O, with 1 min stirring to ensure completely scatter. Next, the slurry was vigorously stirred after the individual additions of TA (1 mL, 6 mM) and Ti-BALDH (10 mL, 6 mM) with 1 min stirring for each addition. Then, the PSS-doped $CaCO_3$ microspheres with $TA\text{-}Ti^{IV}$ coating were washed to remove excess TA and Ti-BALDH. To obtain the $TA\text{-}Ti^{IV}$ microcapsules, the $CaCO_3$ templates were removed by EDTA (50 mM, pH 7.4). Finally, the microcapsules were centrifuged (3058 g, 3 min) and washed with water for three times.

2.4. Preparation of the $TA\text{-}Fe^{III}$ Microcapsules. The preparation process of the $TA\text{-}Fe^{III}$ Microcapsules was mostly in accordance with the literature (slightly modified).[19] The as-prepared PSS-doped $CaCO_3$ was dispersed in 5 mL demineralized H_2O, 2/5 of which was added into 19 mL H_2O, with 1 min stirring to ensure homogeneous distribution. Next, the slurry was vigorously stirred after the individual additions of TA (1 mL, 6 mM) and $FeCl_3$ (3 mL, 6 mM) with 1 min stirring for each addition. Then, 25 mL PBS 8.0 was added to raise the pH value. Finally, the particles were washed to remove excess TA and $FeCl_3$. After these steps, the particles were successfully coated with $TA\text{-}Fe^{III}$. To obtain $TA\text{-}Fe^{III}$ microcapsules, the $CaCO_3$ templates were removed by EDTA (50 mM, pH = 7.4). Finally, the $TA\text{-}Fe^{III}$ microcapsules were centrifuged (3058 g, 3 min) and washed with water three times.

2.5. Preparation of the $TA\text{-}Ti^{IV}$ Microcapsules with CAT. The CAT-PSS-doped $CaCO_3$ microspheres were synthesized via a coprecipitation process according to section 2.2. Specifically, 20 mg CAT was dissolved in 20 mL $CaCl_2$ solution, and then, the same volume of Na_2CO_3 solution with PSS was added and stirred for 30 s at room temperature. The newly synthesized white CAT-PSS-doped $CaCO_3$ microspheres were centrifuged and washed three times. Then, the microspheres were dispersed in 5 mL H_2O, followed by the formation process of the $TA\text{-}Ti^{IV}$ microcapsules the same as that in section 2.3.

2.6. Characterizations. SEM images of the $TA\text{-}Ti^{IV}$ microcapsules were recorded by a field emission scanning electron microscope (Nanosem 430). An energy dispersive spectroscope (EDS) attached to SEM was used to analyze the elemental composition of $TA\text{-}Ti^{IV}$ microcapsules. Atomic force microscopy (AFM) experiment was carried out with a Multimode Nanoscopellla. Confocal laser scanning microscopy (CLSM) images were taken with a Leica TCS SP8 microscope. UV−vis spectra were acquired using a Hitachi U-3010 spectrophotometer. Thermogravimetric analysis (TGA) was performed on a PerkinElmer Pyris analyzer.

All Raman spectra were performed using in Laser Micro-Raman Spectrometer (Thermo Finnigan). TA-Ti sample was dried by freeze-dryer (ALPHR 1−2 LDplus, Germany Christ). All the samples were excited under a He−Ne laser (532 nm). The $TA\text{-}Ti^{IV}$ sample (10.0 mW) was acquired with 10.0 mW incident laser power level and 2.0 s exposure time to partly burn the organic component and form TiO_2. The $TA\text{-}Ti^{IV}$ sample (1.0 mW) was conducted with 1.0 mW incident laser power level and 6.0 s exposure time in order to getting distinct peaks and ensuring the organic undecomposed. The TA sample was under 1.0 mW laser power level and 3.0 s exposure time. Spectral manipulation such as baseline adjustment and smoothing was performed using the omnic 8.0 software.

2.7. UV−vis Absorbance Measurements. The TA and Ti-BALDH solution were mixed with a molar ratio of 1:10, then diluted to suitable concentration to get explicit spectra under UV−vis spectrophotometer before or after coordination reaction. The TA and Ti-BALDH solutions were also diluted to the same concentration for direct comparison.

DOI: 10.1021/acsami.5b01463
ACS Appl. Mater. Interfaces 2015, 7, 9178−9184

2.8. Disassembly Experiments of the TA-Ti^{IV} Microcapsules. The same amount of microcapsules was added into solutions with different pH values (from 1.0 to 13.0) and shaken for 1 h. Then, each kind of the corresponding supernatant was obtained by filter and measured by UV−vis spectrophotometer.

2.9. pH-Stability Experiments of Microcapsules. The stability experiments were carried out in buffer solutions at different pH values (Na_2CO_3−$NaHCO_3$ buffer pH 11.0−9.0; PBS pH 8.0−6.0; CH_3COONa−CH_3COOH pH 5.0−3.0). The buffer solutions containing microcapsules were incubated on a shaker at 800 rpm. After 3 days of incubation, the remaining microcapsules were calculated by cytometer. The remaining efficiency was acquired according to eq 1:

$$\text{remaining efficiency} = \frac{\text{the number of the remaining microcapsules}}{\text{the number of the initial microcapsules}} \times 100\% \quad (1)$$

2.10. Enzyme Encapsulation Efficiency. The amount of immobilized CAT was measured according to Bradford's method.[20] Specifically, the absorbance at 595 nm was measured after mixing 5 mL Coomassie Brilliant Blue reagent with 1 mL supernatant solution for 3 min. The encapsulation efficiency was calculated according to eq 2:

$$\text{encapsulation efficiency (\%)} = \frac{m - C_0V_0 - (C_1V_1 + C_2V_2 + C_3V_3)}{m} \times 100\% \quad (2)$$

Where m (mg) represented the initial weight of CAT; C_0 (mg mL^{-1}), V_0 (mL) represented the enzyme concentration and volume of the supernatant of $CaCO_3$ fabrication process, respectively; C_1, C_2, C_3, and V_1, V_2, V_3 represented the enzyme concentration and volume of the EDTA solutions which were used to remove the $CaCO_3$ templates, respectively.

2.11. Enzyme Activity. The decrease of H_2O_2 absorbance at 240 nm can be utilized to evaluate the free or encapsulated enzyme activity. The H_2O_2 reaction solution (19.6 mM) was prepared in the PBS buffer solution (50 mM, pH 7.0). The TA-Ti^{IV} microcapsules with 0.05 mg CAT were added into 20 mL reaction solution followed by stirring 3 min, and filtered the solution before absorbance measurement. One unit (U) of CAT would decompose 1 μmol of H_2O_2 per minute at pH 7.0 and 25 °C.

2.12. Enzyme Stabilities. For pH stability, the free or encapsulated enzyme was incubated in buffers with various pH values ranging from 4.0 to 9.0 (Na_2CO_3−$NaHCO_3$ buffer pH 9.0; PBS pH 8.0−6.0; CH_3COONa−CH_3COOH pH 5.0−4.0) at 25 °C for 3 h. Afterward, the microcapsules were washed by deionized water three times.

For thermal stability, the free or encapsulated enzyme was incubated under different temperatures ranging from 30 to 70 °C in deionized water for 3 h.

The activities of all the samples were measured according to S11. Then, the relative activity at each specific pH (or temperature) was calculated according to eq 3:

$$\text{relative activity (\%)} = \frac{\text{enzyme activity at specific pH (or temperature)}}{\text{enzyme activity at 30°C, pH 7}} \times 100\% \quad (3)$$

For recycling stability, the microcapsules with CAT were recollected after each reaction batch by membrane separation, and then 20 mL reaction solution was added to fulfill the next reaction cycle. The recycling efficiency of encapsulated CAT was defined as the ratio of the enzyme activity in each reaction cycle to enzyme activity in the first cycle according to eq 4:

$$\text{relative activity (\%)} = \frac{\text{encapsulated enzyme activity in the } n\text{th cycle}}{\text{encapsulated enzyme activity in the 1st cycle}} \times 100\% \quad (4)$$

3. RESULTS AND DISCUSSION

The morphological structure of the TA-Ti^{IV} microcapsules was observed by SEM and AFM. Figure 1a showed that the TA-Ti^{IV} microcapsules were monodispersed and barely fragmented. The diameter of these microcapsules was in the range of 5−8 μm with a relatively smooth surface (Figure 1b). The amplified surface morphology (Figure 1c) of the TA-Ti^{IV} microcapsules was in good accordance with that of dopamine/Ti^{IV} nanoparticles in our previous study.[21] Furthermore, the AFM image (Figure 1d) illustrated that the microcapsules possessed a grainy surface texture with a roughness of R_a = 9.2 ± 0.4 nm and a wall thickness of 15 ± 3 nm. The ultrathin wall is considered to be advantageous for rapid mass transfer. The element composition was measured by energy dispersive spectroscopy (EDS) (Figure S1).

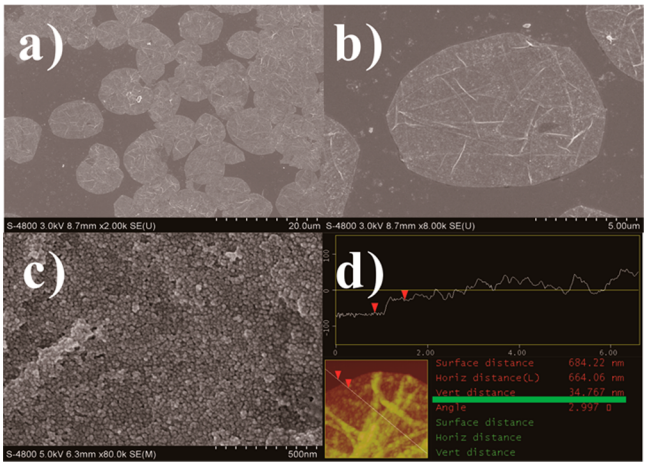

Figure 1. (a−c) SEM images of the TA-Ti^{IV} microcapsules with different magnifications. (d) AFM image of the TA-Ti^{IV} microcapsules.

Quantitative analysis of the TA-Ti^{IV} microcapsules by EDS confirmed the existence of 58.25 at % C, 4.33 at % Ti, and 0.63 at % S. Considering that S only appeared in PSS, the amount of C in PSS was about 5.04 at % which was calculated through stoichiometric ratio of S and C. Then, the amount of C in TA could be obtained through the total amount of C minus the amount of C in PSS. The molar ratio of C (in TA) to Ti was 12:1, equivalently a molar ratio of 1:6 for TA to Ti. Alternatively, the thermogravimetric analysis (TGA) experiment (Figure S2) indicated that the content of inorganic moieties was about 28 wt %, which could be totally assigned to TiO_2. Accordingly, the amount of Ti was calculated to be 16.8 wt %.

The effect of TA and Ti concentrations on the morphology of the resultant microcapsules were further investigated by SEM. Detailed information could be found in Figure S3 and Table S2. The results could be categorized into three groups. For group "*i*", when the TA concentration was kept at a constant value of 0.240 mM, microcapsules could only be obtained beyond a Ti concentration of 2.400 mM (with a molar ratio of 1:10 (TA to Ti)). The stoichiometries in the TA-Ti^{IV} microcapsules were determined by EDS, which is in accordance

DOI: 10.1021/acsami.5b01463
ACS Appl. Mater. Interfaces 2015, 7, 9178−9184

with the molar ratio of TA to Ti in the feed/recipe. For group "*ii*", when the Ti concentrations was kept at a constant value of 2.400 mM, the surface of microcapsules became much rougher and exhibited obvious nanosized particles with the increase of TA concentration as shown in Figure S3a-b and S3e-f. The phenomenon might be ascribed to the following aspect: during the coating formation process, TA at higher concentration quickly coordinates with Ti, which would lead to the generation of nanosized particles, attaching onto the coating surface. For group "*iii*", when the concentrations of TA and Ti both increased along with a fixed molar ratio of 1:10 (TA to Ti), microcapsules can only be formed at a TA concentration of 0.240 mM and a Ti concentration of 2.400 mM. Higher concentrations would result in precipitates rather than microcapsules.

In order to elucidate the formation mechanism of the TA-Ti^{IV} microcapsules, several characterizations and experiments were conducted. As shown in Figure 2a, with the increase of the incident laser intensity from 1.0 to 10.0 mW, the TA-Ti^{IV} microcapsules would be partly oxidized, and several obvious peaks appeared at 152.56, 397.48, 510.29, and 635.64 cm^{-1}. These typical peaks were generally assigned to the Raman shift

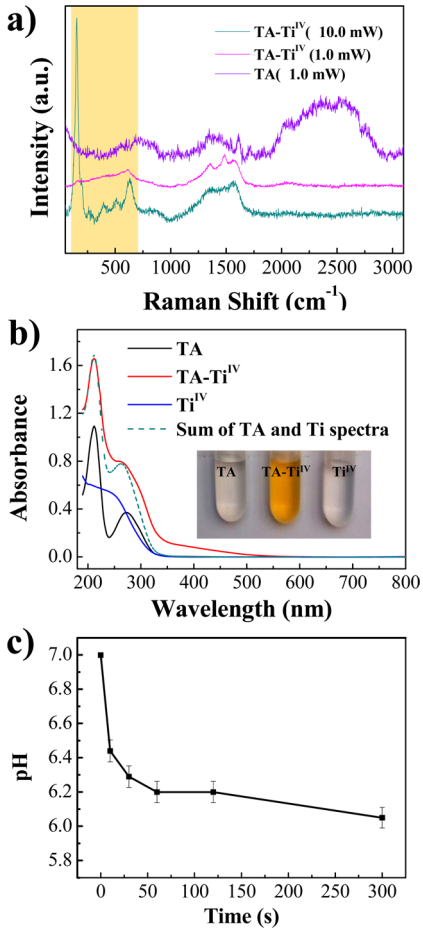

Figure 2. (a) Raman spectra of TA, and the TA-Ti^{IV} microcapsules acquired under different laser intensity. (b) UV−vis spectra of TA, Ti, the mixture of TA and Ti, and the simple summation of the UV−vis spectra of TA and Ti in aqueous solution. (inset) Optical image of TA, Ti, and the mixture of TA and Ti in aqueous solution. (c) Variation of pH values after mixing TA and Ti in aqueous solution as a function of time.

of TiO_2, which indicated that Ti element in the TA-Ti^{IV} microcapsules was in the state of coordination bond rather than TiO_2. The UV−vis spectroscopy was also utilized to monitor the absorbance changes of TA before and after the addition of Ti. It underwent a color switch from colorless to yellow once mixing Ti and TA in aqueous phase. The UV−vis absorbance (Figure 2b) at 435−490 nm well explained the color change phenomenon. Specifically, no UV−vis absorbance can be observed from the TA spectrum, Ti spectrum, and the sum of TA and Ti spectra. By contrast, a broad UV−vis absorbance band at 350−490 nm could be clearly observed for the TA-Ti^{IV} coordination sample. This newly appeared absorbance band was mainly assigned to charge-transfer transition, which was induced by the covalence between the central ion and the ligands.[22] Moreover, suppose that the coordination was formed, numerous H^+ ions in the phenolic hydroxyl groups would be released to the bulk solution, thus increasing the concentration of H^+ ions. Therefore, a pH-monitoring experiment (Figure 2c) was conducted to verify the coordination reaction between TA and Ti (The initial pH values of TA and Ti-BALDH solutions were respectively regulated to 7.0). The pH values decreased with the time prolongation after mixing TA and Ti aqueous solutions, and it reached a plateau after 100 s which meant the termination of the reaction. Collectively, all of the above results indicated that the coordination reaction between TA and Ti indeed occurred.

Since the coordination bond between polyphenol and Ti^{IV} was strong enough against a wide range of pH values, the obtained microcapsules in this study should exhibit weak pH-response. After incubating the same amount of microcapsules into the aqueous solutions with different pH values, the color (Figure 3a) underwent an interesting change. In detail, the suspension was faint yellow at pH < 1, yellow at 3.0 < pH < 11.0, reddish-yellow at pH > 13.0. The UV−vis absorbance of the supernatant was also measured to detect the coordination state and the disassembly behavior of the TA-Ti^{IV} microcapsules. The similar UV−vis spectra of the samples incubated at pH 3, 5, 7, 9, and 11 suggested no or slight structural changes of these TA-Ti^{IV} microcapsules. The spectrum of pH = 13.0 showed big absorption bands at 224 and 286 nm, indicating the complete disassembly of the microcapsules. Meanwhile, the absorbance between 350 and 500 nm indicated that the TA-Ti^{IV} coordination bond still existed, but in a state of bis μ-oxo, $[Ti^{IV}O(polyphenol)]_2^{4-}$ (Figure 3b and S5).[15,16] Even if at pH 1.0, the tiny absorbance suggested slight disassembly of TA-Ti^{IV} microcapsules. The biggest absorption bands for the curve of pH = 1.0 were located at 212, 252, and 362 nm. Under such extremely acidic condition, the coordination state might be $[Ti^{IV}(polyphenol)_2$ (H polyphenol)$]_2^{2-}$ (Figure 3b and S7) evidenced by the color change and the shift of peak positions.[23] This kind of structure still kept tris-coordination state and five chelate rings, ensuring it more stable than other metal ions which became mono- or bis-coordination compound with one or two chelate rings. Figure 3c showed a more intuitive information about the pH-responsive properties of the microcapsules. Generally, few TA-Ti^{IV} microcapsules were disassembled after 3 day-incubation in a pH range of 3−11, which was in accordance with the UV−vis result. By contrast, the TA-Fe^{III} microcapsules can only retain their intact structure under a much narrower pH range (pH 5−8).[13] Particularly, once changing the pH of the incubation solution to 10.0, a black precipitate was observed for the TA-Fe^{III} microcapsules, which might be $Fe(OH)_3$. Additionally, the TA-Ti^{IV} micro-

DOI: 10.1021/acsami.5b01463
ACS Appl. Mater. Interfaces 2015, 7, 9178−9184

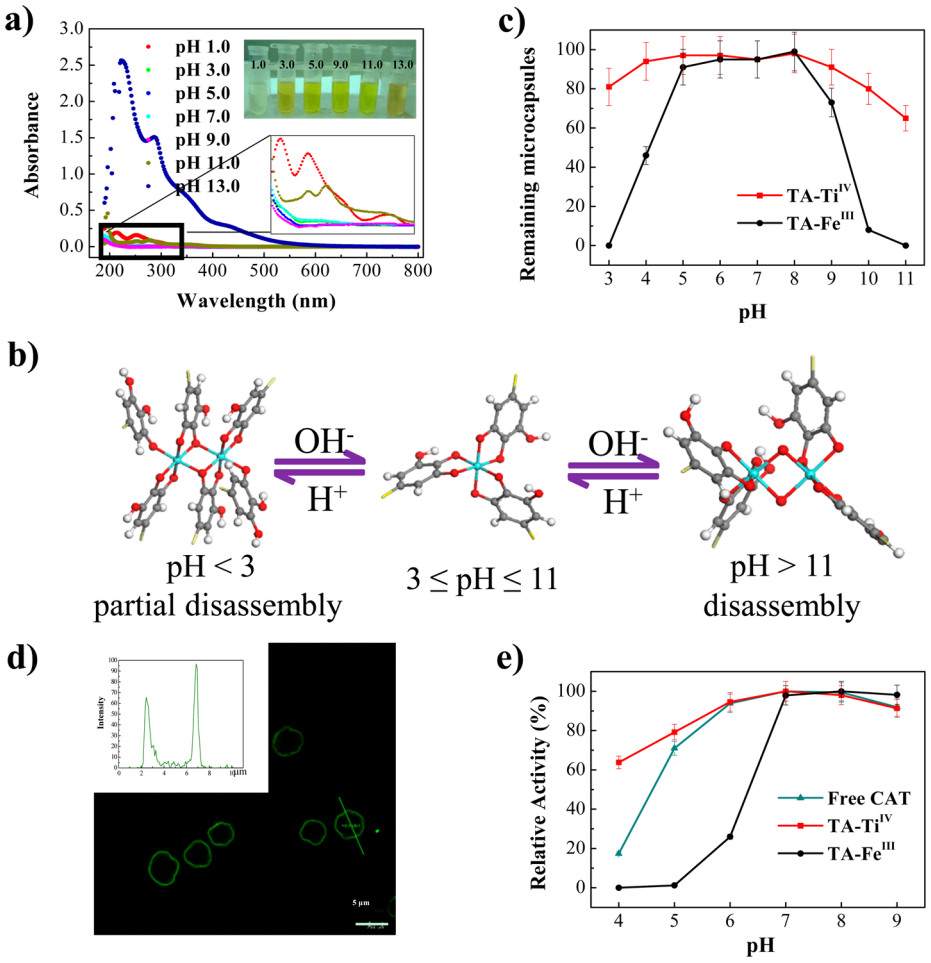

Figure 3. (a) UV−vis spectra of the TA-Ti^{IV} microcapsules supernatant at various pH values. (inset lower right) Enlarged view. (inset upper right) Optical image of the TA-Ti^{IV} microcapsules in aqueous solution at different pH values. (b) Switching of TA-Ti^{IV} coordination state at different pH values. Ti, O, C, H, and Fe atoms are represented by blue, red, gray, white, and purple spheres, respectively. The remainder of TA molecule is represented by yellow sticks. (c) pH-disassembly behavior of the TA-Ti^{IV} and the TA-Fe^{III} microcapsules in aqueous solution at different pH values. (d) CLSM image of the TA-Ti^{IV} microcapsules containing FITC-CAT. The inset is the fluorescence intensity profile along the line crossing the microcapsule. (e) pH stability of free enzyme, the TA-Ti^{IV} and TA-Fe^{III} microcapsules with CAT.

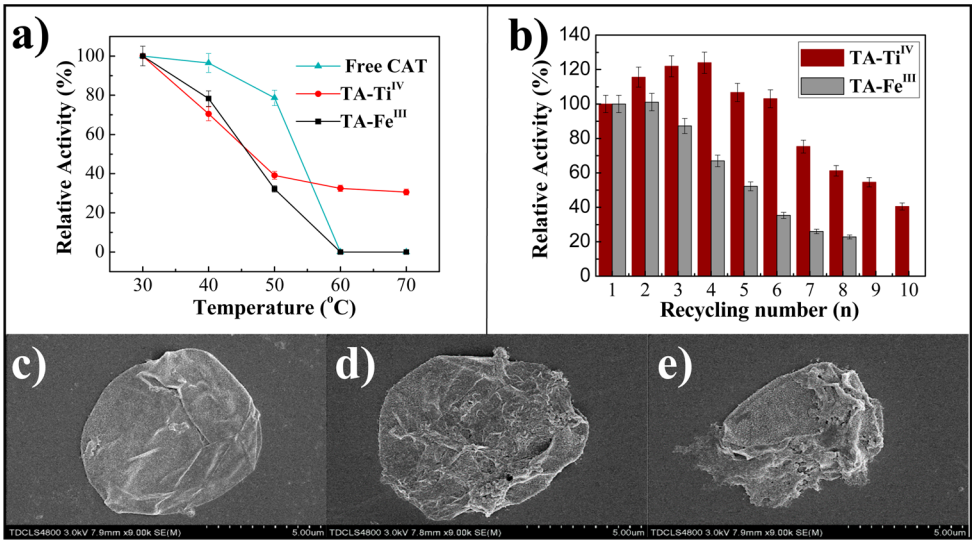

Figure 4. (a) Thermal stability of the free enzyme, the TA-Ti^{IV} microcapsules with CAT, and the TA-Fe^{III} microcapsules with CAT. (b) Recycling stability of the TA-Ti^{IV} microcapsules with CAT and the TA-Fe^{III} microcapsules with CAT. SEM images of the TA-Ti^{IV} microcapsules with CAT (c) before reaction, (d) after the 5th cycle reaction, and (e) after the 10th cycle reaction.

DOI: 10.1021/acsami.5b01463
ACS Appl. Mater. Interfaces 2015, 7, 9178−9184

capsules displayed good structural stability even in the presence of EDTA (date not shown), a commonly used chelating reagents, further verifying the robustness of the TA-Ti^{IV} coordination bond.

As is well-known, microcapsule is one of the most efficient carriers for enzyme immobilization because both the capsule lumen and the capsule wall can load enzymes and well retain the three-dimensional structure of enzyme molecules.[24] Ultrathin microcapsules with weak pH-responsive property are particularly anticipated in the application of enzyme catalysis mainly owing to the following two aspects: (1) low substrate/product transfer resistance would lead to a higher enzyme catalytic activity and (2) a robust capsule wall would bring a desirable stability against harsh conditions. Herein, catalase (CAT) as a model enzyme was immobilized in the TA-Ti^{IV} microcapsules for conducting the enzyme catalysis (detailed immobilization procedure can be found in the Experimental Section). The TA-Ti^{IV} microcapsules showed an immobilization efficiency[25] of ~93% with an enzyme activity of 320 units mg^{-1}. To trace the location of enzyme within the microcapsules, FITC-labeled CAT was immobilized in the TA-Ti^{IV} microcapsules. As show in Figure 3d, the CAT molecules were primarily enriched on the microcapsule wall due to the interaction between enzyme and TA which may be arisen from the Michael addition or Schiff base reaction (Figure S8−9) between the amine groups in enzyme molecule and quinone group in TA,[21] or the hydrogen bond formed between enzyme molecule and TA. Once utilized for converting H_2O_2, the TA-Ti^{IV} microcapsules with CAT showed a superior pH stability in a broad range of pH values as shown in Figure 3e. In detail, under acidic conditions (pH 4.0), the TA-Ti^{IV} microcapsules with CAT could maintain a relative activity of 62% in accordance with Figure 3a and c. In comparison, the breakage of the TA-Fe^{III} microcapsules at lower pH could cause the enzyme leaking during washing step, further leading to a rather weak pH stability of the immobilized enzyme. This pH-responsive disassembly property restricted the application of the TA-Fe^{III} microcapsules in catalysis, which also highlighted the importance of exploring weak pH-responsive microcapsules.

Other relevant stabilities such as the recycling stability and thermal stability of the TA-Ti^{IV} microcapsules with CAT were also conducted. The thermal stability (Figure 4a) result showed that the TA-Ti^{IV} and TA-Fe^{III} microcapsules with CAT exhibited similar relative activity at 30 to 50 °C. At a higher temperature, the TA-Ti^{IV} microcapsules maintained desirable performance because the titanium materials could prevent enzyme molecule from thermal denaturation.[21] The recycling stability results (Figure 4b−e) indicated that the TA-Ti^{IV} microcapsules with CAT outperformed the TA-Fe^{III} microcapsules with CAT because of the stronger TA-Ti^{IV} coordination bond.

4. CONCLUSION

In conclusion, the ultrathin TA-Ti^{IV} microcapsules with high stability in a broad range of pH values were prepared through coordination-enabled one-step assembly upon hard-templating process. These microcapsules preserved their intact wall structure under extreme acidic/alkaline conditions owing to the robust coordination bonding between TA and Ti^{IV}. Once utilized for enzyme immobilization, the TA-Ti^{IV} microcapsules displayed the high catalytic performance, especially the superior pH and thermal stabilities. In particular, this study demonstrates that the binding of catechols with Ti^{IV} is stronger than that of Fe^{III}, and therefore TA-Ti^{IV} are more stable in the pH scale. This finding should have important implications for materials science and catalysis.

■ ASSOCIATED CONTENT

Supporting Information

Additional experimental data including the coordination stability of different metal ions; EDS and TGA result of the TA-Ti^{IV} microcapsules; SEM images and results of various TA and Ti concentrations; the probable structure; the recycling and thermal stability. This material is available free of charge via the Internet at http://pubs.acs.org.

■ AUTHOR INFORMATION

Corresponding Authors

*E-mail: zhyjiang@tju.edu.cn. Fax: +86-22-27406646. Tel.: +86-22-27406646 (Z.J.).

*E-mail: shijiafu@tju.edu.cn. Fax: +86-22-27890566. Tel.: +86-22-27890566 (J.S.).

Notes

The authors declare no competing financial interest.

■ ACKNOWLEDGMENTS

The authors thank the National Science Fund for Distinguished Young Scholars (21125627), National Natural Science Funds of China (21406163), the Program of Introducing Talents of Discipline to Universities (B06006), Specialized Research Fund for the Doctoral Program of Higher Education (No. 20130032110023), and Program for New Century Excellent Talents in University (No. NCET-10-0623) for financial support.

■ REFERENCES

(1) Such, G. K.; Johnston, A. P. R.; Liang, K.; Caruso, F. Synthesis and Functionalization of Nanoengineered Materials Using Click Chemistry. *Prog. Polym. Sci.* **2012**, *37*, 985−1003.

(2) Such, G. K.; Johnston, A. P.; Caruso, F. Engineered Hydrogen-bonded Polymer Multilayers: from Assembly to Biomedical Applications. *Chem. Soc. Rev.* **2011**, *40*, 19−29.

(3) Trojer, M. A.; Nordstierna, L.; Nordin, M.; Nydén, M.; Holmberg, K. Encapsulation of actives for sustained release. *Phys. Chem. Chem. Phys.* **2013**, *15*, 17727−17741.

(4) Trojer, M. A.; Nordstierna, L.; Bergek, J.; Blanck, H.; Holmberg, K.; Nydén, M. Use of microcapsules as controlled release devices for coatings. *Adv. Colloid Interface Sci.* **2014**, DOI: 10.1016/j.cis.2014.06.003.

(5) Yang, M.; Ma, J.; Zhang, C. L.; Yang, Z. Z.; Lu, Y. F. General Synthetic Route toward Functional Hollow Spheres with Double-shelled Structures. *Angew. Chem., Int. Ed.* **2005**, *44*, 6727−6730.

(6) Ariga, K.; Lvov, Y. M.; Kawakami, K.; Ji, Q.; Hill, J. P. Layer-by-layer Self-assembled Shells for Drug Delivery. *Adv. Drug Delivery Rev.* **2011**, *63*, 762−71.

(7) Ariga, K.; McShane, M.; Lvov, Y. M.; Ji, Q. M.; Hill, J. P. Layer-by-layer Assembly for Drug Delivery and Related Applications. *Expert Opin. Drug Del.* **2011**, *8*, 633−644.

(8) Shi, J.; Zhang, W.; Wang, X.; Jiang, Z.; Zhang, S.; Zhang, X.; Zhang, C.; Song, X.; Ai, Q. Exploring the Segregating and Mineralization-inducing Capacities of Cationic Hydrophilic Polymers for Preparation of Robust, Multifunctional Mesoporous Hybrid Microcapsules. *ACS Appl. Mater. Interfaces* **2013**, *5*, 5174−85.

(9) Crespy, D.; Stark, M.; Hoffmann-Richter, C.; Ziener, U.; Landfester, K. Polymeric Nanoreactors for Hydrophilic Reagents Synthesized by Interfacial Polycondensation on Miniemulsion Droplets. *Macromolecules* **2007**, *40*, 3122−3135.

DOI: 10.1021/acsami.5b01463
ACS Appl. Mater. Interfaces 2015, 7, 9178−9184

(10) Yu, A. M.; Wang, Y. J.; Barlow, E.; Caruso, F. Mesoporous Silica Particles as Templates for Preparing Enzyme-loaded Biocompatible Microcapsules. *Adv. Mater.* **2005**, *17*, 1737−1741.
(11) Liu, P. Stabilization of Layer-by-layer Engineered Multilayered Hollow Microspheres. *Adv. Colloid Interface Sci.* **2014**, *207*, 178−188.
(12) Wilhelm, K. P.; Zhai, H.; Maibach, H. I. *Dermatotoxicology*; CRC Press: Boca Raton, 2010.
(13) Ejima, H.; Richardson, J. J.; Liang, K.; Best, J. P.; van Koeverden, M. P.; Such, G. K.; Cui, J.; Caruso, F. One-step Assembly of Coordination Complexes for Versatile Film and Particle Engineering. *Science* **2013**, *341*, 154−7.
(14) Novio, F.; Simmchen, J.; Vazquez-Mera, N.; Amorin-Ferre, L.; Ruiz-Molina, D. Coordination Polymer Nanoparticles in Medicine. *Coord. Chem. Rev.* **2013**, *257*, 2839−2847.
(15) Sever, M. J.; Wilker, J. J. Visible Absorption Spectra of Metal-catecholate and Metal-tironate Complexes. *Dalton Trans.* **2004**, 1061−72.
(16) Sever, M. J.; Wilker, J. J. Absorption Spectroscopy and Binding Constants for First-row Transition Metal Complexes of a DOPA-containing Peptide. *Dalton Trans.* **2006**, 813−22.
(17) Sunkara, B.; Misra, R. Enhanced Antibactericidal Function of W^{4+}-doped Titania-coated Nickel Ferrite Composite Nanoparticles: A Biomaterial System. *Acta Biomater.* **2008**, *4*, 273−283.
(18) Shi, J.; Yang, C.; Zhang, S.; Wang, X.; Jiang, Z.; Zhang, W.; Song, X.; Ai, Q.; Tian, C. Polydopamine Microcapsules with Different Wall Structures Prepared by a Template-mediated Method for Enzyme Immobilization. *ACS Appl. Mater. Interfaces* **2013**, *5*, 9991−7.
(19) Guo, J.; Ping, Y.; Ejima, H.; Alt, K.; Meissner, M.; Richardson, J. J.; Yan, Y.; Peter, K.; von Elverfeldt, D.; Hagemeyer, C. E.; Caruso, F. Engineering Multifunctional Capsules through the Assembly of Metal-phenolic Networks. *Angew. Chem., Int. Ed.* **2014**, *53*, 5546−51.
(20) Bradford, M. M. A Rapid and Sensitive Method for the Quantitation of Microgram Quantities of Protein Utilizing the Principle of Protein-dye Binding. *Anal. Biochem.* **1976**, *72*, 248−54.
(21) Yang, C.; Wu, H.; Shi, J. F.; Wang, X. L.; Xie, J. L.; Jiang, Z. Y. Preparation of Dopamine/Titania Hybrid Nanoparticles through Biomimetic Mineralization and Titanium(IV)-Catecholate Coordination for Enzyme Immobilization. *Ind. Eng. Chem. Res.* **2014**, *53*, 12665−12672.
(22) Gispert, J. R. *Coordination Chemistry*; Wiley: Hoboken, 2008.
(23) Borgias, B. A.; Cooper, S. R.; Koh, Y. B.; Raymond, K. N. Synthetic, Structural, and Physical Studies of Titanium Complexes of Catechol and 3, 5-di-tert-butylcatechol. *Inorg. Chem.* **1984**, *23*, 1009−1016.
(24) Patwardhan, S. V.; Patwardhan, G.; Perry, C. C. Interactions of Biomolecules with Inorganic Materials: Principles, Applications and Future Prospects. *J. Mater. Chem.* **2007**, *17*, 2875−2884.
(25) Sheldon, R. A.; van Pelt, S. Enzyme Immobilisation in Biocatalysis: Why, What and How. *Chem. Soc. Rev.* **2013**, *42*, 6223−35.

DOI: 10.1021/acsami.5b01463
ACS Appl. Mater. Interfaces 2015, 7, 9178−9184